Shape Constraint Strategies: Novel Approaches and Comparative Robustness

Juan J. Cerrolaza
juanjose.cerrolaza@unavarra.es
Arantxa Villanueva
avilla@unavarra.es
Rafael Cabeza
rcabeza@unavarra.es

Biomedical Engineering Group,
Department of Electrical and
Electronics Engineering.
Public University of Navarra.
Navarra, SPAIN

Since their inception in the early nineties with the seminal work of Cootes et al. [5], Active Shape Models (ASMs) have become one of the most popular segmentation paradigms, thanks to their robustness and versatility. Basically, the ASM algorithm can be described as an iterative process in which two statistical models are sequentially applied to drive the segmentation process. A statistical appearance model guides the matching process of the shape to a new image, whereas a statistical model of shape imposes shape restrictions defining a subspace of allowed shapes (SAS). The SAS must be sufficiently restrictive to prevent the appearance of incoherent cases, but also general enough to include new, valid, unseen shapes.

In the context of ASM, the vectorial expression of each instance of the shape space, $\mathbf{x}$, is created by concatenating the coordinates of the K d-dimensional landmarks used to described it. Each shape is approximated by the linear equation $\mathbf{x} = \bar{\mathbf{x}} + \mathbf{P}\mathbf{b}$, where $\bar{\mathbf{x}}$ is the mean shape and the vector $\mathbf{b} = (b_1, b_2, ..., b_t)^T$ is the expression of the shape in the new coordinate system defined by the t main eigenvectors of the covariance matrix of the training set, $\mathbf{P} = (\mathbf{p}_1 \mid \mathbf{p}_2 \mid ... \mid \mathbf{p}_t)$. One of the most simplest and most widespread techniques to guarantee that only plausible instances are generated is to apply hard limits independently to each component of $\mathbf{b}$, with $\mid b_j \mid \leq \beta\sqrt{\lambda_j}$ $(j = 1, \ldots, t)$, approximating the SAS to a hyperrectangle, $\mathbf{b} \simeq \mathbf{b}_{HR}$ (see Figure 1). The parameter β is a constant that determines the flexibility of the model, typically between 1 and 3. However, this very simple approximation can lead to highly unlikely instances, such as those in which every component takes the extreme value $\pm\beta\sqrt{\lambda_j}$. A more accurate representation of the SAS can be obtained if considering the different instances of the shape are distributed according to a multivariate normal distribution, defining a hyperelliptical constant potential surface as $(\sum_{j=1}^{t} \frac{b_j^2}{\beta^2\lambda_j}) - 1 = 0$. Instead of calculating the point of the hyperellipsoid closest to $\mathbf{b}$, the constraint method proposed by Stegmann [4] consists of simply scaling those shape vectors out of the SAS, correcting $\mathbf{b}$ by $\mathbf{b}_S$ (see Figure 1). Although this approximation prevents the occurrence of such highly imporbable instances as those allowed by the hyperrectangular approximation, it can cause undesirable collateral deformations that negatively affect the segmentation process.

In this work, a new, efficient hyperelliptical approximation of the SAS is presented. Suppose $\mathbf{b}_{HE}$ represents that point over the hyperellipsoid "surface" closest to $\mathbf{b}$. This can be expressed by the following system of equations,

$$\begin{cases} (\sum_{j=1}^{t} \frac{b_{HE,j}^2}{\beta^2\lambda_j}) - 1 = 0 \\ \\ \min\left(\sum_{j=1}^{t}(b_{HE,j} - b_j)^2\right) \end{cases} \quad (1)$$

Both equations can be combined into the following single objective function to optimise

$$F(\mathbf{b}_{HE}, \alpha) = \sum_{j=1}^{t}(b_{HE,j} - b_j)^2 + \alpha\left(\left(\sum_{j=1}^{t}\frac{b_{HE,j}^2}{\beta^2\lambda_j}\right) - 1\right) \quad (2)$$

which can be easily and efficiently solved by the Newton-Raphson method.

Next to the presentation of this new hyperelliptical fitting method, the other main goal of this paper is the introduction of a detailed and rigorous experimental study that makes it possible to evaluate the actual differences between alternative shape constraint techniques, paying attention not only to the accuracy but also the effect on other configuration parameters and the potential interactions between them. In particular, the values considered for each parameter are as follows: four values for β (1.5, 2, 2.5, 3); seven different lengths for the appearance profile γ, expressed in pixels to each side of the landmark (3, 4, 5, 6, 7, 8, 9); and four search ranges in the landmark updating process, δ, expressed as pixels to each side of the full appearance profile (2, 3, 4, 5), for a total of 112 different parameters configurations. The three factor analysis of variance model [2] that express the effect that these parameters of factors have over the final response of the algorithm can be defined as $y_{ijkn} = \mu + \mu_{\beta_i} + \mu_{\gamma_j} + \mu_{\delta_k} + \mu_{\beta\gamma_{ij}} + \mu_{\beta\delta_{ik}} + \mu_{\gamma\delta_{jk}} + \mu_{\beta\gamma\delta_{ijk}} + \varepsilon_{ijkl}$, where $i = 1, \ldots, 4$, $j = 1, \ldots, 7$, $k = 1, \ldots, 4$, and $n = 1, \ldots, N$; y_{ijkn} is the segmentation error of the $ijkn$-th observation; μ is the overall mean common to all cases; μ_{β_i}, μ_{γ_j} and μ_{δ_k} represent the main effect of the i, j and k - th tested value of the factors β, γ and δ respectively; $\mu_{\beta\gamma_{ij}}$, $\mu_{\beta\delta_{ik}}$ and $\mu_{\gamma\delta_{jk}}$ reflect the interaction effect between pairs of factors and $\mu_{\beta\gamma\delta_{ijk}}$ is the interaction between all of them; and ε_{ijkl} is the random error component of the $ijkn$-th observation. The subindex n corresponds to the n-th shape tested.

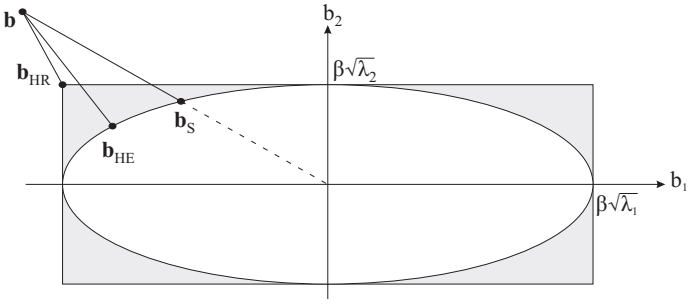

Figure 1: A graphical illustration (for the simplified case where $t = 2$) of three different shape constraint strategies. $\mathbf{b}_{HR}$, $\mathbf{b}_S$ and $\mathbf{b}_{HE}$ represent the corrections provided by the hyperrectangle projection, the scaling proposed by Stegmann [4] and the new hyperelliptical approximation respectively.

Using two different databases, the AR facial database [1] and the JSRT chest radiographs database [3], the results provided by this general factorial design demonstrate how the use of the new hyperelliptical fitting not only improves the average segmentation accuracy but also the robustness of the algorithm to variations of the configuration settings, especially of the flexibility of the statistical model, which is directly linked to the SAS approach used. On the other hand, the F-test performed at the typical 5% significance level revealed the absence of interaction effects between the parameters, a result of crucial importance in the optimisation of the segmentation process.

[1] Aleix Martínez and Robert Benavente. The AR face database. Technical report, Computer Vision Center, Universitat Autònoma de Barcelona, 1998. (Available from http://www2.ece.ohio-state.edu/ aleix/ARdatabase.html).

[2] Douglas C. Montgomery. *Design and Analysis of Experiments*. John Wiley and Sons, 2004. ISBN 047148735X.

[3] J. Shiraishi, S. Katsuragawa, J. Ikezoe, T. Matsumoto, T. Kobayashi, K. Komatsu, M. Matsui, H. Fujita, Y. Kodera, and K. Doi. Development of a digital image database for chest radiographs with and without a lung nodule: receiver operating characteristic analysis of radiologists' detection of pulmonary nodules. *American Journal of Roentgenology*, 174:71–74, 2000.

[4] M. B. Stegmann, R. Fisker, and B. K. Ersbøll. On properties of active shape models. Technical report, Informatics and Mathematical Modelling, Technical University of Denmark, DTU, Richard Petersens Plads, Building 321, DK-2800 Kgs. Lyngby, 2000.

[5] C. J. Taylor, D. H. Cooper, and J. Graham. Training models of shape from sets of examples. In *Proc. Brit. Mach. Vision Conf.*, pages 9–18, 1992.